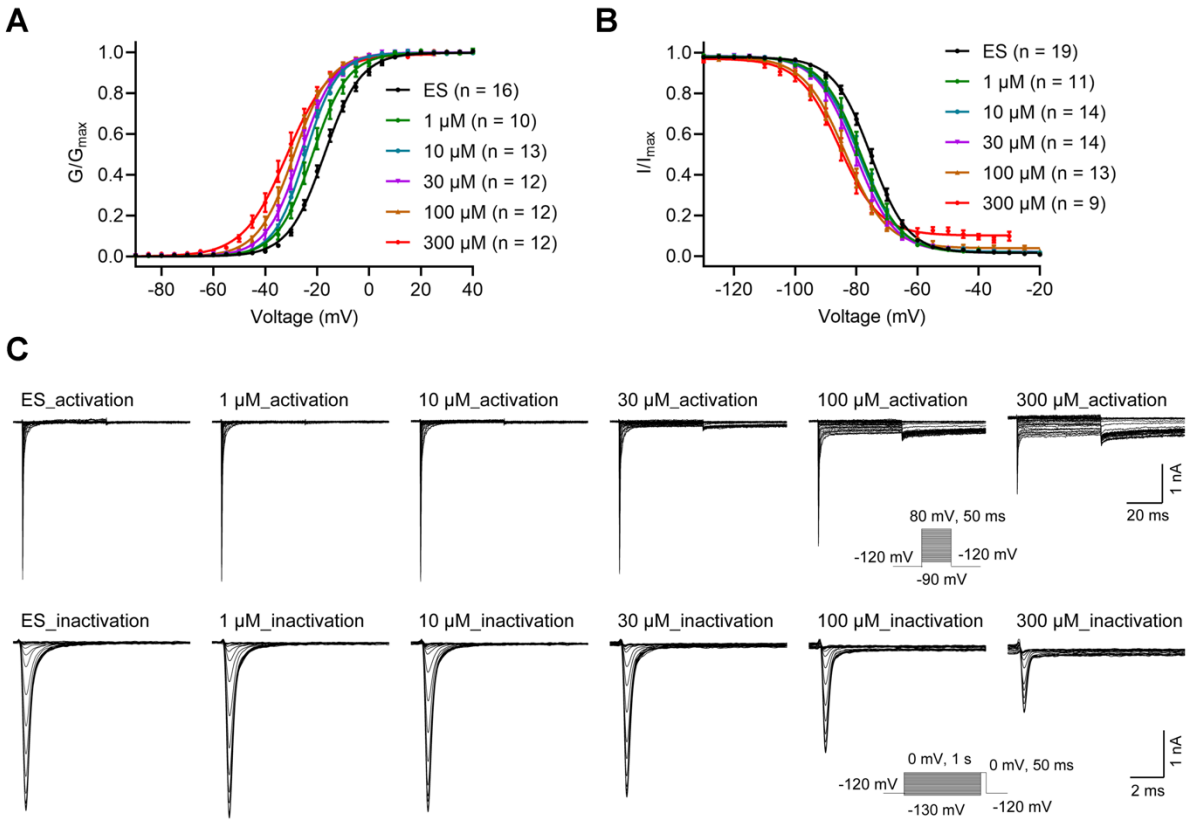

Figure S1 | Functional characterizations of veratridine modulation on human $Na_v1.7$. (**A**) Voltage-dependent activation curves and (**B**) steady-state inactivation curves of $Na_v1.7$ recorded under varying concentrations of veratridine. (**C**) Representative current traces illustrating voltage-dependent activation (*top*) and steady-state inactivation (*bottom*) of $Na_v1.7$ in the presence of veratridine at the indicated concentrations. Inserts are the recording protocols.

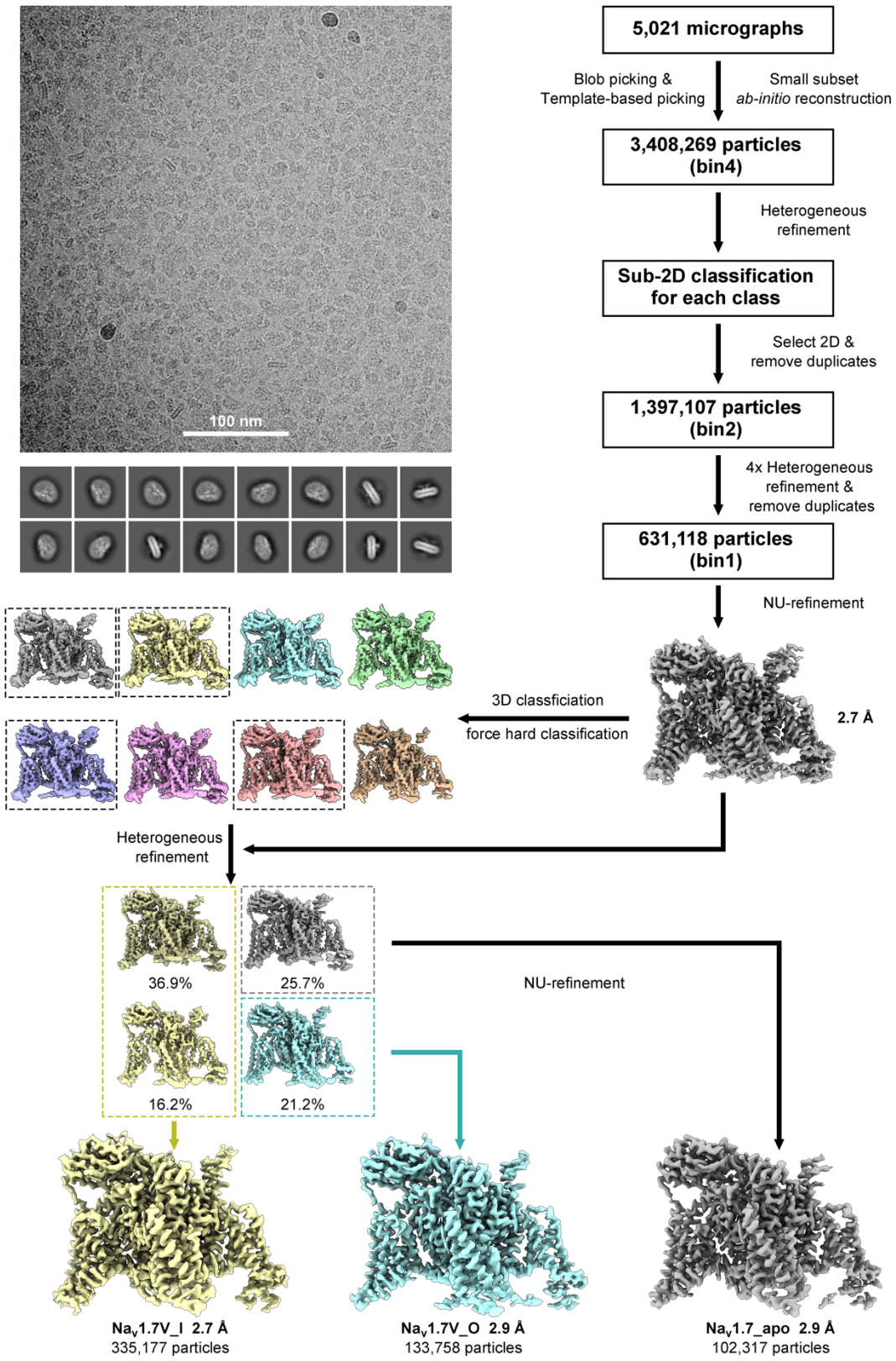

Figure S2 | Workflow for cryo-EM data processing. A representative raw micrograph and corresponding 2D class averages are presented. Related details are provided in *Materials and Methods*.

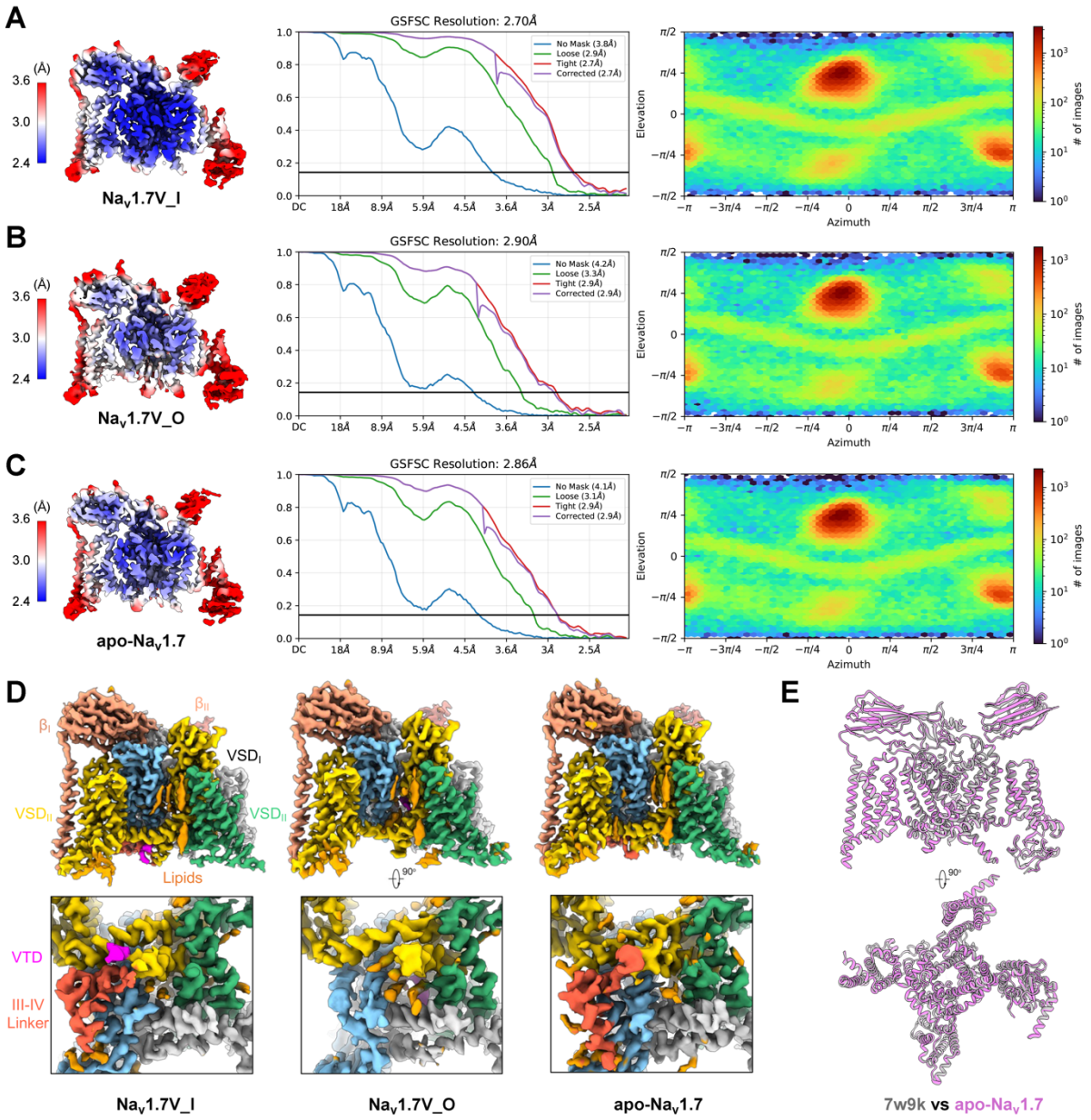

Figure S3 | Cryo-EM analysis of the Na$_v$1.7-VTD complex reveals three distinct classes. (**A-C**) Local resolution estimations (*left*), gold-standard Fourier shell correlation (GS-FSC) curves (*middle*), and angular distributions (*right*) for classes Na$_v$1.7V_I (**A**), Na$_v$1.7V_O (**B**), and apo-Na$_v$1.7 (**C**), respectively. (**D**) Overall cryo-EM 3D reconstructions (*top*) and corresponding zoomed-in views of the intracellular gate (*bottom*), highlighting the distinct ligand-binding features in each class. (**E**) Structural superposition revealed that the apo-Na$_v$1.7 class closely matches the previously reported apo structure (PDB: 7w9k), with an RMSD of 0.60 Å over 1,235 Cα atoms.

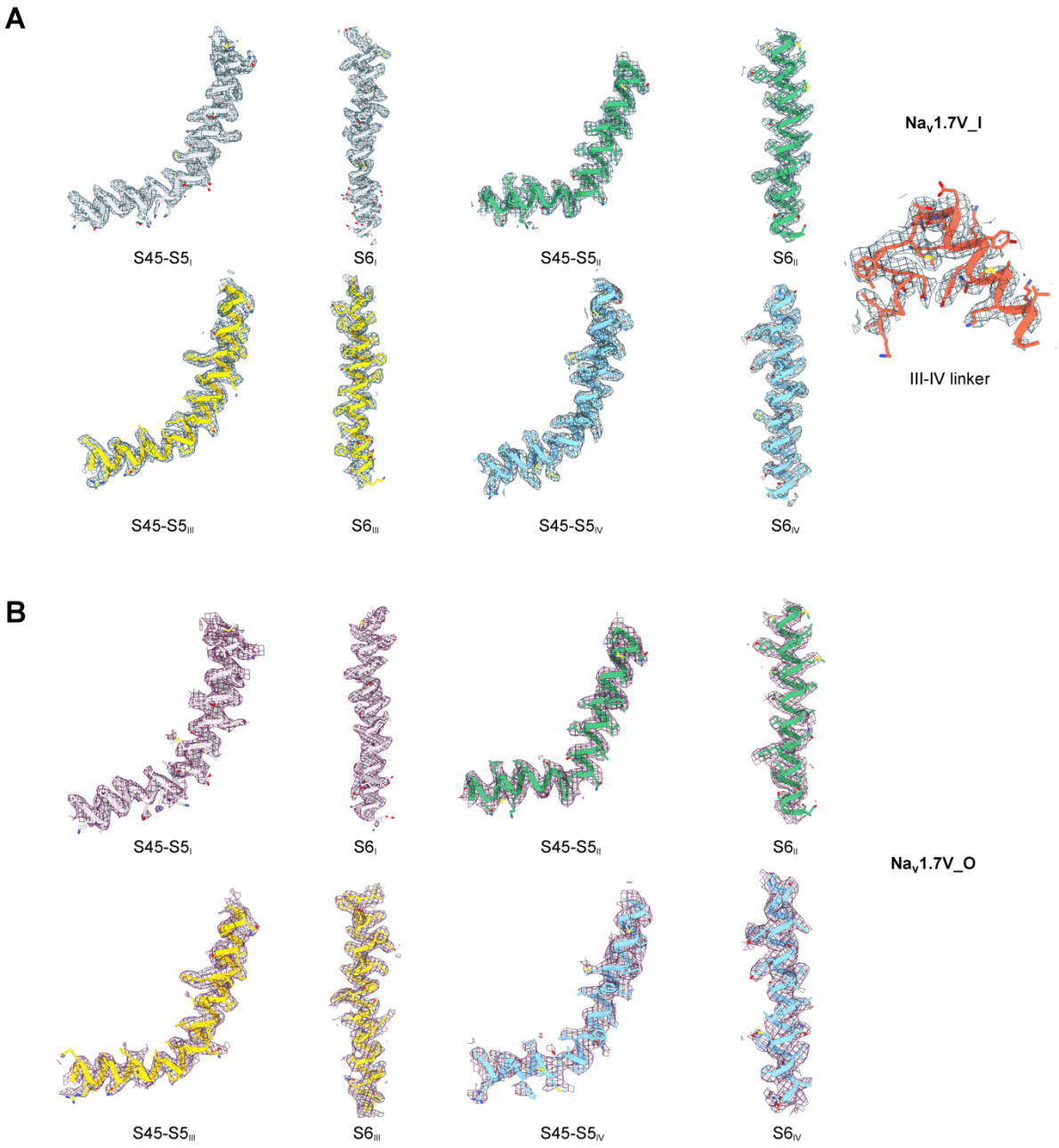

Figure S4 | Local cryo-EM densities of the $Na_v1.7$-VTD pore domains. Shown are the local pore-domain helix densities for (**A**) $Na_v1.7V\_I$ class, and (**B**) $Na_v1.7V\_O$ class, each exhibiting well-resolved features that corroborate the reconstructed maps and corresponding atomic models.

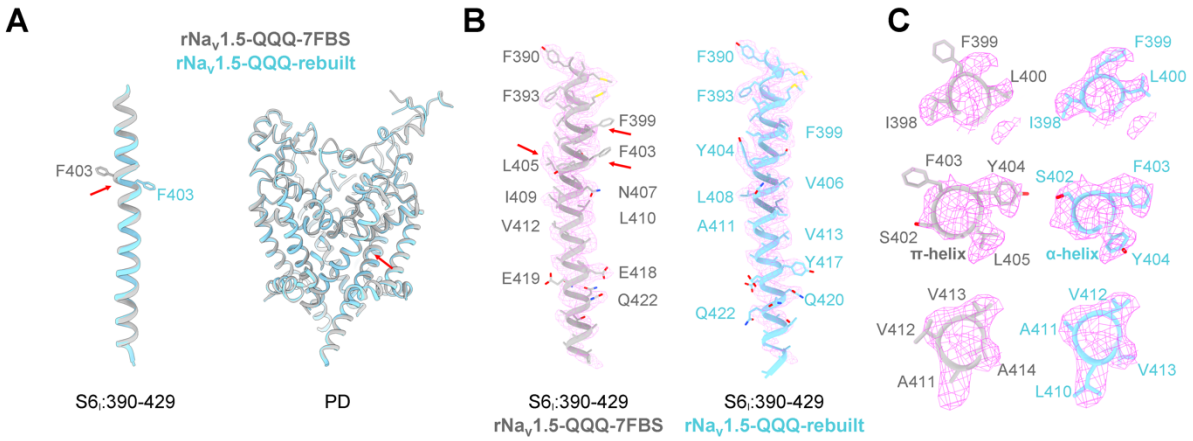

D

	rNaV1.5-QQQ-7FBS	rNaV1.5-QQQ-rebuilt
Protein residues	606	606
RMSD Bond lengths (Å)	0.010	0.003
RMSD Bond angles (°)	1.159	0.545
MolProbity score	2.66	1.23
Clashscore	16.74	4.56
Rotamer outliers (%)	3.75	0.79
CaBLAM outliers (%)	3.41	0.68
Ramachandran plot		
Favored (%)	91.61	98.15
Allowed (%)	8.22	1.85
Disallowed (%)	0.17	0.00

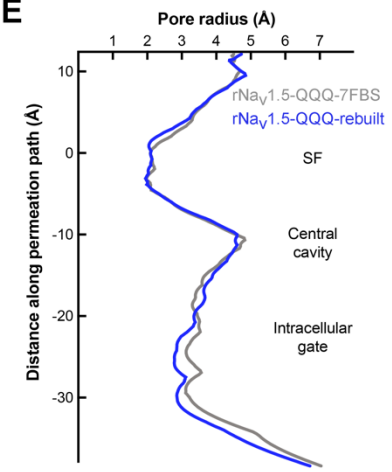

Figure S5 | Validation and refinement of the rNa$_V$1.5-QQQ model. (**A**) Superposition of the original (PDB:7FBS, grey) and rebuilt (cyan) pore-domain structures of rNa$_V$1.5-QQQ. The most significant change is the rebuilt α-helix spanning residues 400-403 within the S6$_I$ segment (*left*). Red arrows indicate the origin of the assignment error. (**B**) Model-to-density fit for the original and rebuilt rNa$_V$1.5-QQQ S6$_I$ segments within the deposited EM map (EMD-31519). Red arrows highlight examples of poorly fitted side chains in the original model that were corrected during refinement. (**C**) Close-up views of the S6$_I$ helix fit at each turn. The rebuilt model (cyan) shows improved density agreement, supporting an α-helical conformation at Phe403 instead of the previously assigned π-helix. (**D**) Quantitative metrics of model validation support the improved quality of the refined model. (**E**) Ion permeation path analysis indicates subtle alterations to the conduction path in the refined model compared to the original structure.

Table S1 | Parameters of the concentration-response relationships for veratridine-mediated inhibition of peak currents and enhancement of accumulated tail currents in $hNa_v1.7$.

Parameters	**inhibition of peak currents**		**enhancement of accumulated tail current**	
IC_{50} / EC_{50} (μM)	92.66 ± 18.41		95.44 ± 16.62	
k (mV)	1.06 ± 0.18		0.82 ± 0.12	
Top	0.80 ± 0.11		0.85 ± 0.12	
[VTD]	Mean ± SEM	n	Mean ± SEM	n
0 μM	/	/	0.013 ± 0.004	18
1 μM	0.005 ± 0.021	13	0.023 ± 0.004	10
10 μM	0.052 ± 0.017	17	0.112 ± 0.006	12
30 μM	0.201 ± 0.021	16	0.252 ± 0.011	13
100 μM	0.405 ± 0.028	15	0.416 ± 0.019	13
300 μM	0.620 ± 0.023	15	0.626 ± 0.037	11

Each data point represents mean ± s.e.m (standard deviation of mean), and n denotes the number of independently recorded cells.

Table S2 | Parameters of voltage-dependent activation and steady-state inactivation of hNa$_v$1.7 with and without veratridine.

	Parameters	ES	1 μM	10 μM	30 μM	100 μM	300 μM
voltage-dependent activation	$V_{1/2}$ (mV)	-17.21 ± 0.21	-21.77 ± 0.34 ****	-24.50 ± 0.21 ****	-26.45 ± 0.30 ****	-28.93 ± 0.37 ****	-31.68 ± 0.50 ****
	P	/	<0.0001	<0.0001	<0.0001	<0.0001	<0.0001
	k (mV)	7.00 ± 0.18	6.84 ± 0.29	6.17 ± 0.18 **	6.68 ± 0.26	7.03 ± 0.31	8.46 ± 0.43 ***
	P	/	0.5992	0.0013	0.2959	0.9420	0.0004
	n	16	10	13	12	12	12
steady-state inactivation	$V_{1/2}$ (mV)	-75.29 ± 0.23	-78.51 ± 0.40 ****	-79.28 ± 0.36 ****	-80.39 ± 0.36 ****	-83.69 ± 0.42 ****	-85.54 ± 0.53 ****
	P	/	<0.0001	<0.0001	<0.0001	<0.0001	<0.0001
	k (mV)	-6.06 ± 0.20	-6.41 ± 0.35	-6.54 ± 0.32	-6.42 ± 0.32	-6.83 ± 0.37 *	-6.63 ± 0.47
	P	/	0.3524	0.1792	0.3115	0.0488	0.2136
	n	19	11	14	14	13	9

*P < 0.05, **P < 0.01, ***P < 0.001, ****P < 0.0001 versus Na$_v$1.7 on the condition of external solution. The extra sum-of-squares F test was used to compare the $V_{1/2}$ and slope factor (*k*) of both activation and inactivation. Each data point represents mean ± s.e.m (standard deviation of mean) and n is the number of independently recorded cells. ES, external solution.

Table S3 | Statistics for cryo-EM data and structural refinement.

	$Na_v1.7V\_I$	$Na_v1.7V\_O$
Data collection and processing		
Magnification	105,000	105,000
Voltage (kV)	300	300
Electron dose (e-/Å^2)	50	50
Defocus range (μm)	-1.2~-1.6	-1.2~-1.6
Pixel size (Å)	1.114	1.114
Symmetry	C1	C1
Total good particle	631,118	631,118
Final particles	335,177	133,758
Map resolution (Å)	2.7	2.9
FSC threshold	0.143	0.143
Refinement		
Map sharpening *B* factor (Å^2)	103.9	101.6
Model composition		
Non-hydrogen atoms	13,103	12,531
Protein residues	1,538	1,472
Ligands	26	25
B factors (Å^2)		
Protein	65.92	99.95
Ligand	110.59	116.04
R.m.s deviations		
Bond lengths (Å)	0.003	0.002
Bond angles (^{o})	0.527	0.499
Validation		
MolProbity score	1.39	1.37
Clashscore	7.15	6.80
Rotamer outliers (%)	0.22	0.08
CaBLAM outliers (%)	0.80	0.77
Ramachandran plot		
Favored (%)	98.69	98.69
Allowed (%)	1.31	1.31
Disallowed (%)	0.00	0.00